Sum rules of electromagnetic response functions in ^{12}C

Alessandro Lovato

In collaboration with:
Stefano Gandolfi, Ralph Butler, Joseph Carlson, Ewing Lusk,
Steven C. Pieper, and Rocco Schiavilla.

**Argonne**
NATIONAL LABORATORY

Introduction

- The electroweak resp[onse] ingredient to describe carbon scattering, re[c] MiniBooNE collabora[tion] detector aimed at stu[dying] oscillations.

  Excess, at relatively low energy, of measured cross section relative to theoretical calculations.

- As a first step towards its calculation, we have computed the sum rules for the electromagnetic response of 12C. We want to predict the results of Jefferson lab experiment nearing publication.
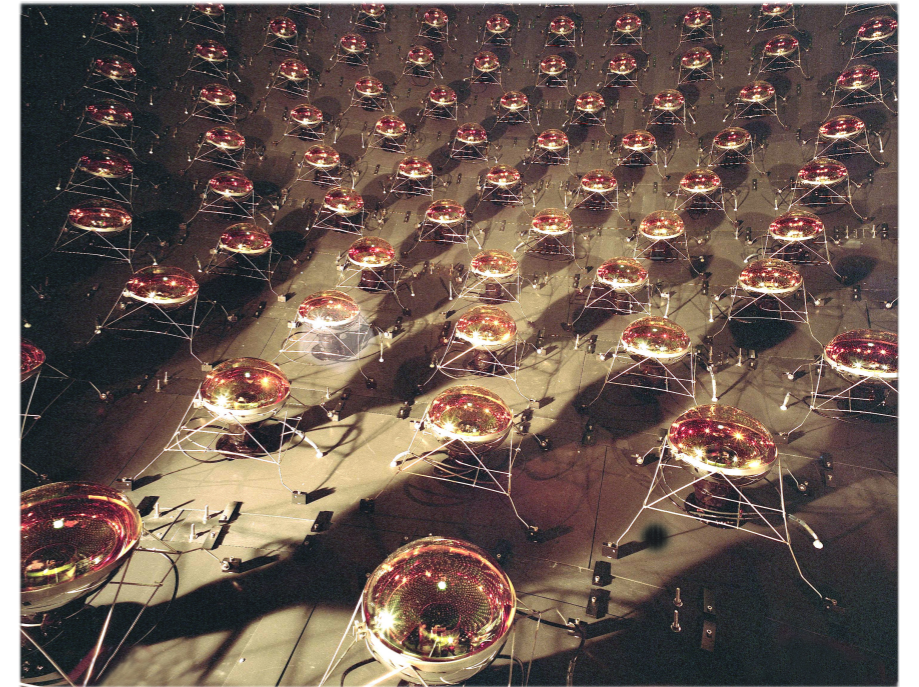
Electromagnetic response

The electromagnetic <u>inclusive</u> cross section of the process

$$e + {}^{12}C \rightarrow e' + X$$

where the target final state is <u>undetected</u>, can be written in the Born approximation as
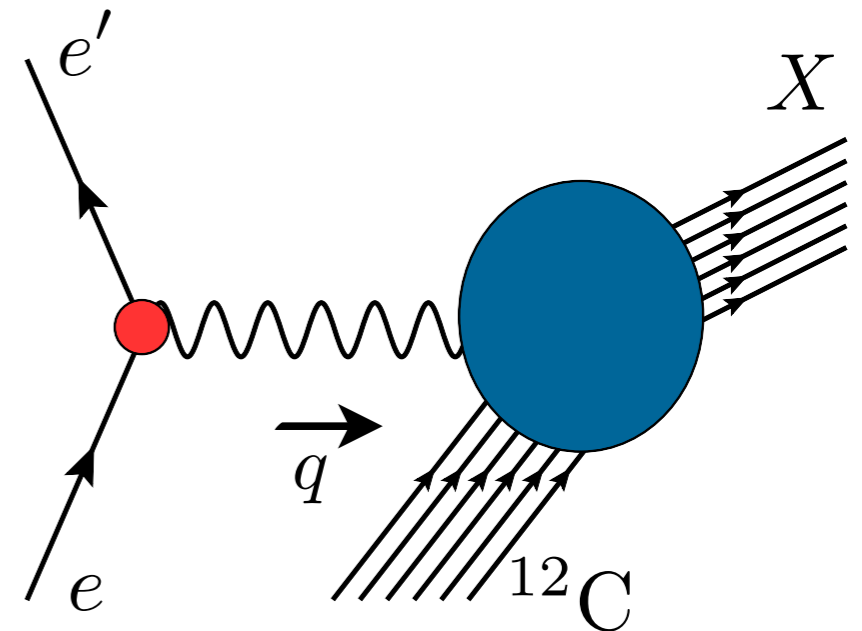
$$\frac{d^2\sigma}{d\Omega_{e'} dE_{e'}} = -\frac{\alpha^2}{q^4} \frac{E_{e'}}{E_e} L_{\mu\nu} W^{\mu\nu} \ ,$$

The <u>leptonic tensor</u> is fully specified by the measured electron kinematic variables

$$L_{\mu\nu} = 2[k_\mu k'_\nu + k_\nu k'_\mu - g_{\mu\nu}(kk')]$$
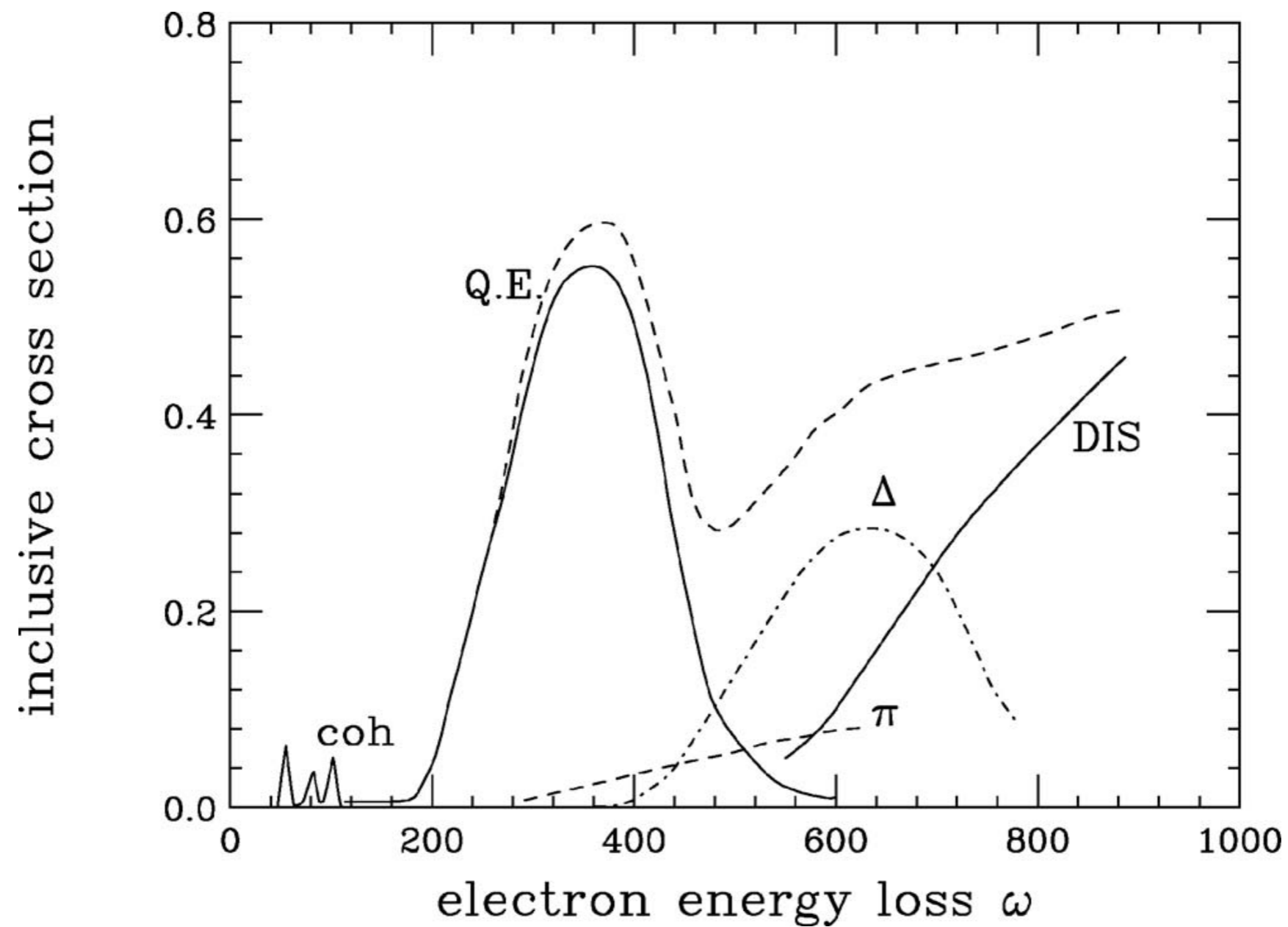
The <u>Hadronic tensor</u> contains all the information on target structure.

$$W^{\mu\nu} = \sum_X \langle \Psi_0 | J^\mu | \Psi_X \rangle \langle \Psi_X | J^\nu | \Psi_0 \rangle \delta^{(4)}(p_0 + q - p_X)$$

Electromagnetic response

Schematic representation of the inclusive cross section.

Electromagnetic response

• At moderate momentum transfer, non relativistic wave functions can be used to describe the initial and final states and an expansion of the current operator in powers of $|\mathbf{q}|/m$ can be performed.

• The hadronic tensor (and the cross section) can be written in terms of the longitudinal and transverse response functions, with respect to the direction of the three-momentum transfer:

Longitudinal
$$R_L(q,\omega) = \sum_X \langle \Psi_0 | \rho | \Psi_X \rangle \langle \Psi_X | \rho | \Psi_0 \rangle \delta(E_0 + \omega - E_X)$$

Transverse
$$R_T(q,\omega) = \sum_X \langle \Psi_0 | \vec{j}_T^\dagger | \Psi_X \rangle \langle \Psi_X | \vec{j}_T | \Psi_0 \rangle \delta(E_0 + \omega - E_X)$$
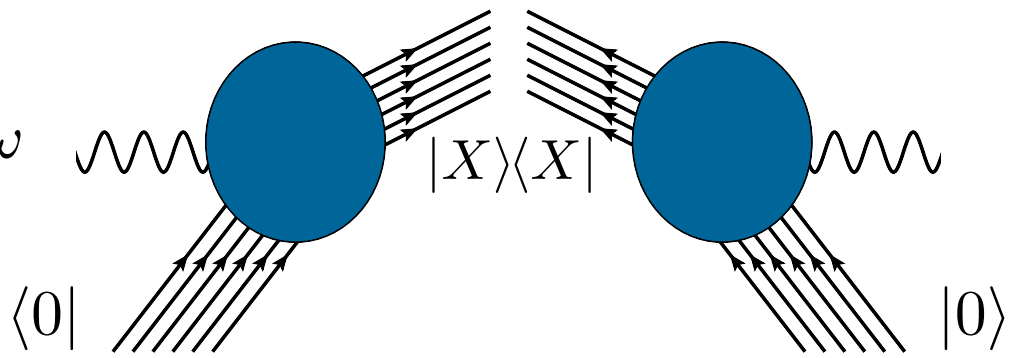
• Realistic models for the electromagnetic charge and current operators include one- and two-body terms, the latter assumed to be due to exchanges of effective pseudo-scalar and vector mesons.

Electromagnetic sum rules

- The direct calculation of the response requires the knowledge of all the transition amplitudes: $\langle \Psi_0 | \rho | \Psi_X \rangle$ and $\langle \Psi_0 | \vec{j}_T | \Psi_X \rangle$.

- The <u>sum rules</u> provide an useful tool for studying integral properties of the electron-nucleus scattering.

$$S_\alpha(q) = C_\alpha \int_{\omega_{\text{th}}^+}^{\infty} d\omega \, \frac{R_\alpha(q,\omega)}{G_E^{p\,2}(Q^2)}$$

Proton electric form factor

- Using the completeness relation, they can be expressed as <u>ground-state expectation values of the charge and current operators</u>.

$$S_\alpha(q) \; \boldsymbol{=} \; \sum_X \int d\omega$$

Longitudinal and transverse sum rules.

Longitudinal sum rule

$$S_L(\mathbf{q}) = C_L \left[\frac{1}{G_E^p(Q_{qe}^2)} \langle 0|\rho(\mathbf{q})\rho(\mathbf{q})|0\rangle - \frac{1}{G_E^p(Q_{el}^2)} |\langle 0; \mathbf{q}|\rho(\mathbf{q})|0\rangle|^2 \right] \quad ; \quad C_L = \frac{1}{Z}$$

The elastic contribution, proportional to the longitudinal form factor has been removed.

$$F_L(\mathbf{q}) = C_L \langle 0; \mathbf{q}|\rho(\mathbf{q})|0\rangle$$

Transverse sum rule

$$S_T(\mathbf{q}) = \frac{C_T}{G_E^p(Q_{qe}^2)} \langle 0|\vec{j}_T^\dagger(\mathbf{q})\vec{j}_T(\mathbf{q})|0\rangle \quad ; \quad C_T = \frac{2}{\left(Z\,\mu_p^2 + N\,\mu_n^2\right)} \frac{m^2}{q^2}$$

• C_L and C_T have been introduced under in order for $S_\alpha(q \to \infty) \longrightarrow 1$ in the approximation where nuclear charge and current operators originate solely from the charge and spin magnetization of individual protons and neutrons and that relativistic corrections are ignored.

Comparison with experiment

Direct comparison between the calculated and experimentally extracted sum rules cannot be made unambiguously for two reasons

- The experimental determination of S_α requires measuring the associated R_α in the whole energy-transfer region, from threshold up to . ∞

Inclusive electron scattering experiments only allow access to the region where $\omega < q$

Extrapolation needed
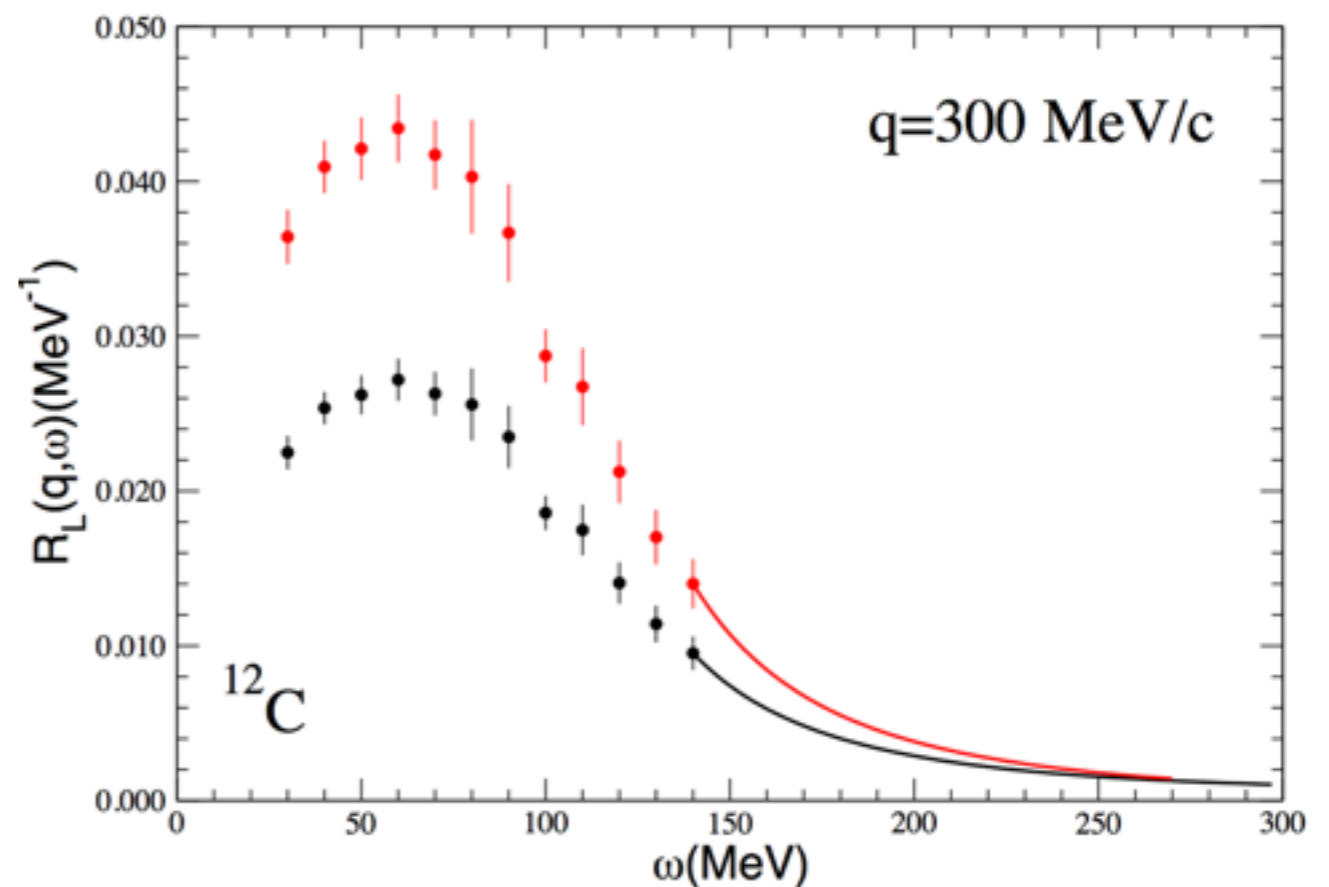
- Inadequacy of the dynamical framework to account for explicit pion production mechanisms.

Ab-initio few-nucleon calculation

- The density and current operators have to be consistent with the _realistic_ nucleon-nucleon (NN) interaction.

$$\textbf{Argonne v}_{18}: \qquad v_{18}(r_{12}) = \sum_{p=1}^{18} v^p(r_{12}) \hat{O}_{12}^p$$

is controlled by ~4300 np and nn scattering data below 350 MeV of the Nijmegen database.

- Static part $\quad \hat{O}_{ij}^{p=1-6} = (1, \sigma_{ij}, S_{ij}) \otimes (1, \tau_{ij})$ $\qquad$ Deuteron, S and D wave phase shifts

- Spin-orbit $\quad \hat{O}_{ij}^{p=7-8} = \mathbf{L}_{ij} \cdot \mathbf{S}_{ij} \otimes (1, \tau_{ij})$ $\qquad$ P wave phase shifts

$$\begin{cases} \mathbf{L}_{ij} = \dfrac{1}{2i}(\mathbf{r}_i - \mathbf{r}_j) \times (\mathbf{\nabla}_i - \mathbf{\nabla}_j) \quad \longleftrightarrow \qquad \text{Angular momentum} \\[2em] \mathbf{S}_{ij} = \dfrac{1}{2}(\boldsymbol{\sigma}_i + \boldsymbol{\sigma}_j) \qquad\qquad\qquad\quad\longleftrightarrow \quad \text{Total spin of the pair} \end{cases}$$

The remaining operators are needed to achieve the description of the Nijmegen scattering data with $\chi^2 \simeq 1$. They accounts for quadratic spin-orbit interaction and charge symmetry breaking effects.

Ab-initio few-nucleon calculation

• To compute the sum rules and the longitudinal form factor, the ground state wave function of ^{12}C needs to be precisely known. An accurate three body potential has to be introduced.
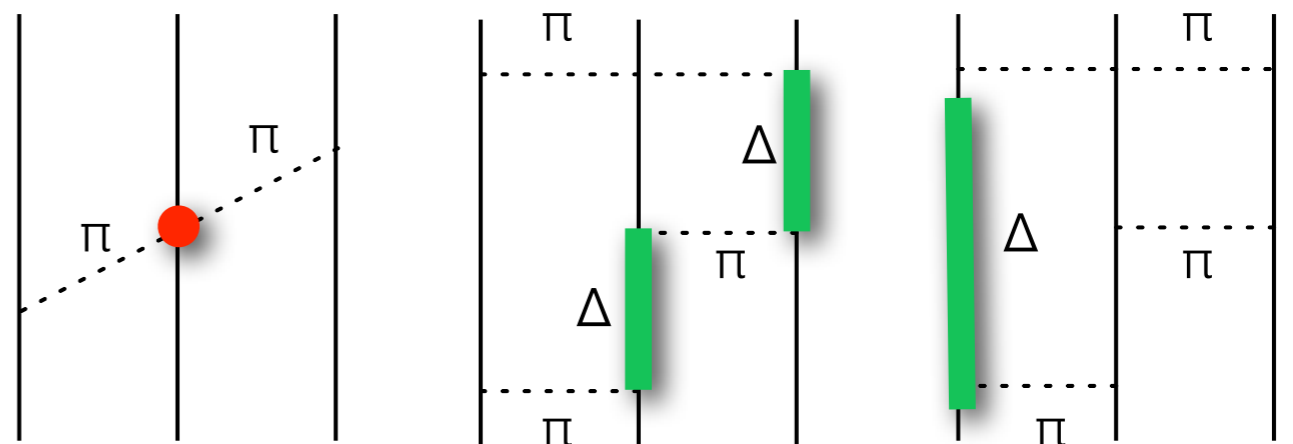
Urbana IX

contains the attractive Fujita and Miyazawa two-pion exchange interaction and a phenomenological repulsive term.
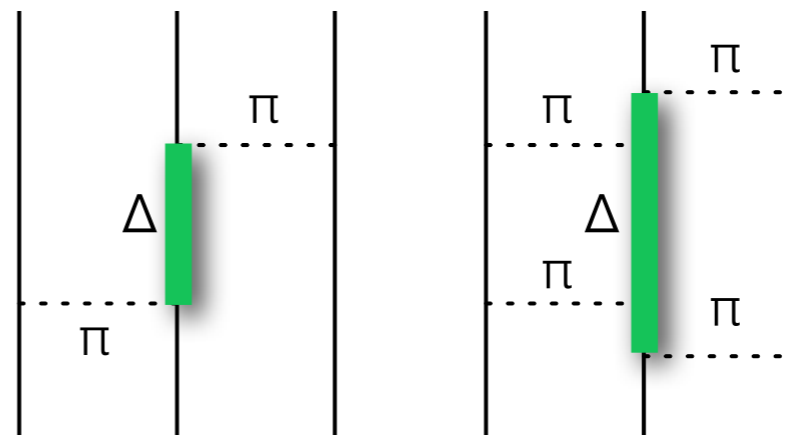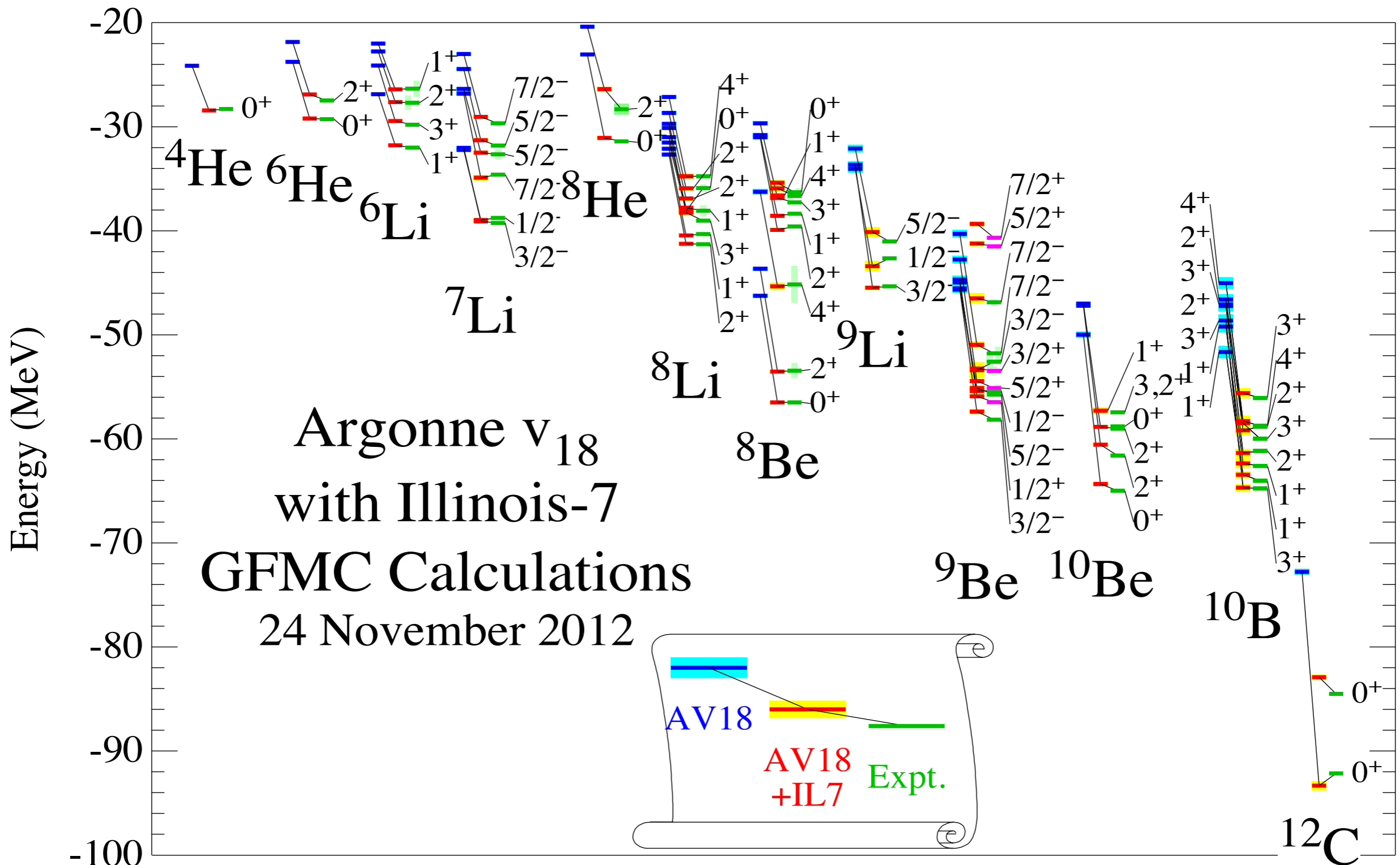
Illinois 7

also includes terms originating from three-pion exchange diagrams and the two-pion S-wave contribution.

We have used Illinois 7 potential, that can be written as

$$V_{ijk} = A_{2\pi}^{PW} O_{ijk}^{2\pi,PW} + A_{2\pi}^{SW} O_{ijk}^{2\pi,SW} + A_{3\pi}^{\Delta R} O_{ijk}^{3\pi,\Delta R} + A_R O_{ijk}^R .$$

Ab-initio few-nucleon calculation

Green's Function Monte Carlo

Solving the many body Schroedinger equation is made particularly difficult by the complexity of the interaction, which is spin-isospin dependent and contains strong tensor terms

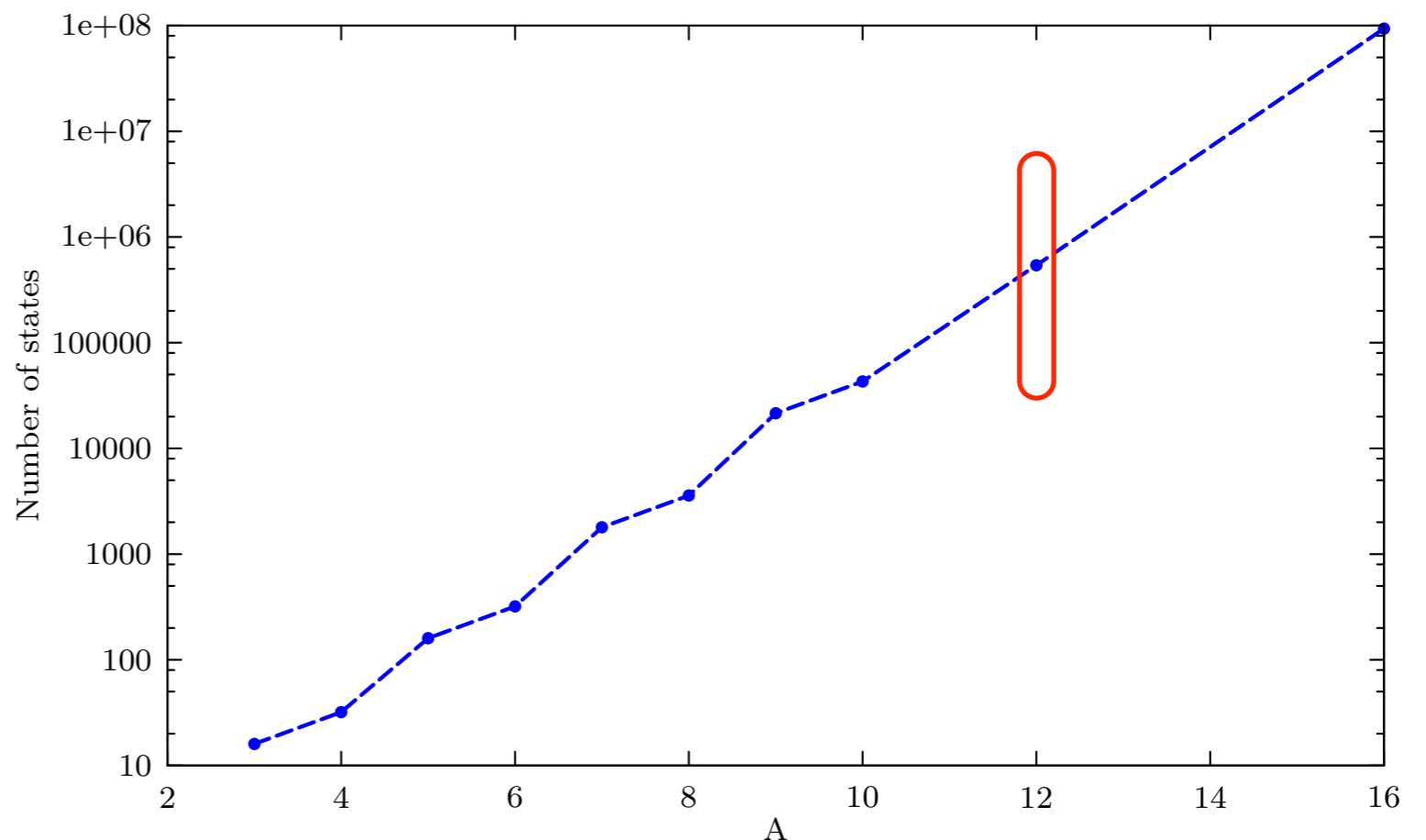$$\hat{H}\Psi_0(x_1 \ldots x_A) = E_0\Psi_0(x_1 \ldots x_A)$$

The wave function can be expresses as a sum over spin-isospin states

$$\Psi_0(x_1 \ldots x_A) = \sum_{\alpha=1}^{N} \Psi_0(\mathbf{r}_1 \ldots \mathbf{r}_A)|\alpha\rangle$$

the number of which grows exponentially with the number of particles

$$N = 2^A \times \binom{A}{Z}$$

For ^{12}C **270,336** second order coupled differential equations in 36 variables !!!

Green's Function Monte Carlo

GFMC algorithms use projection techniques to enhance the ground-state component of a starting trial wave function

$$\Psi_0(x_1 \ldots x_A) = \lim_{\tau \to \infty} e^{-(\hat{H}-E_0)\tau} \Psi_T(x_1 \ldots x_A)$$

The trial wave function contains 3-body correlations stemming from 3-body potential

$$\Psi_T = \left[1 + \sum_{i<j<k} \tilde{U}_{ijk}^{TNI}\right]\Psi_P \qquad \longleftrightarrow \qquad \tilde{U}_{ijk} = \tilde{\epsilon}_A V_{ijk}^A + \epsilon_R V_{ijk}^R$$

The pair correlated wave function is written in terms of operator correlations

$$\Psi_P = \left[\mathcal{S}\sum_{i<j}(1 + U_{ij})\right]\Psi_J \qquad \longleftrightarrow \qquad U_{ij} = \sum_{p=2,6}\left[\prod_{k\neq j,i} f^p(\mathbf{r}_{ik}, \mathbf{r}_{jk})\right]u_p(r_{ij})O_{ij}^p$$

Since the operators do not commute, their ordering is sampled

The total antisymmetric Jastrow wave function depends on the nuclear state.

$$\Psi_J = \left[\prod_{i<j<k} f_{ijk}^c\right]\left[\prod_{i<j} f_{ij}^c\right]\Phi_A(J, M, T, T_3) \qquad \longleftrightarrow \qquad \Phi_4(0,0,0,0) = \mathcal{A}|p\uparrow p\downarrow n\uparrow n\downarrow\rangle$$

⁴He

Green's Function Monte Carlo

- Within GFMC the wave function is represented by a complex vector of $2^A \binom{A}{Z}$ numbers, each depending on the 3A coordinates: a GFMC sample.

- The ³H case fits in the slide!

$$|\Psi_{^3H}\rangle = \begin{pmatrix} a_{\uparrow\uparrow\uparrow} \\ a_{\uparrow\uparrow\downarrow} \\ a_{\uparrow\downarrow\uparrow} \\ a_{\uparrow\downarrow\downarrow} \\ a_{\downarrow\uparrow\uparrow} \\ a_{\downarrow\uparrow\downarrow} \\ a_{\downarrow\downarrow\uparrow} \\ a_{\downarrow\downarrow\downarrow} \end{pmatrix} \qquad \hat{\sigma}_{12}|\Psi_{^3H}\rangle = \begin{pmatrix} a_{\uparrow\uparrow\uparrow} \\ a_{\uparrow\uparrow\downarrow} \\ 2a_{\downarrow\uparrow\uparrow} - a_{\uparrow\downarrow\uparrow} \\ 2a_{\downarrow\uparrow\downarrow} - a_{\uparrow\downarrow\downarrow} \\ 2a_{\uparrow\downarrow\uparrow} - a_{\downarrow\uparrow\uparrow} \\ 2a_{\uparrow\downarrow\downarrow} - a_{\downarrow\uparrow\downarrow} \\ a_{\downarrow\downarrow\uparrow} \\ a_{\downarrow\downarrow\downarrow} \end{pmatrix}$$

Green's Function Monte Carlo

Each imaginary time step consists in a 3A dimensional integral, evaluated within the Monte Carlo approach.

$$G_{\alpha\beta}(\mathbf{R}, \mathbf{R}') =_{\alpha} \langle \mathbf{R}|e^{-(\hat{H}-E_0)\Delta\tau}|\mathbf{R}'\rangle_{\beta} \quad \longleftrightarrow \quad \text{Matrix in spin-isospin space!}$$

The short-time propagator is constructed from the exact two-body propagator

$$G_{\alpha\beta}(\mathbf{R}, \mathbf{R}') = G_0(\mathbf{R}, \mathbf{R}')_{\alpha}\langle\Big[\mathcal{S}\prod_{i<j}\frac{g_{ij}(\mathbf{r}_{ij}, \mathbf{r}'_{ij})}{g_{0\,,ij}(\mathbf{r}_{ij}, \mathbf{r}'_{ij})}\Big]\rangle_{\beta}$$
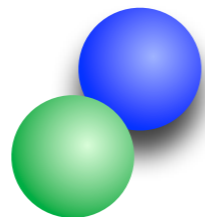
which is given by

$$g_{ij}(\mathbf{r}_{ij}, \mathbf{r}'_{ij}) = \langle\mathbf{r}_{ij}|e^{-\hat{H}_{ij}\Delta\tau}|\mathbf{r}'_{ij}\rangle \quad \longleftrightarrow \quad \hat{H}_{ij} = -\frac{\nabla^2_{ij}}{m} + \hat{v}_{ij}$$

while $g_{0\,,ij}(\mathbf{r}_{ij}, \mathbf{r}'_{ij})$ is the free two-body propagator. Using the exact two-body propagators allows for larger time steps:
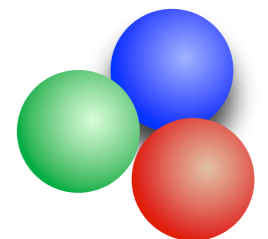
Standar Trotter

Large error if two particles are very close $\sim v_{ij}\hat{T}v_{ij}\Delta\tau^3$

Two-body propagator

Large error if three particles are very close $\sim v_{ij}\hat{T}v_{ik}\Delta\tau^3$
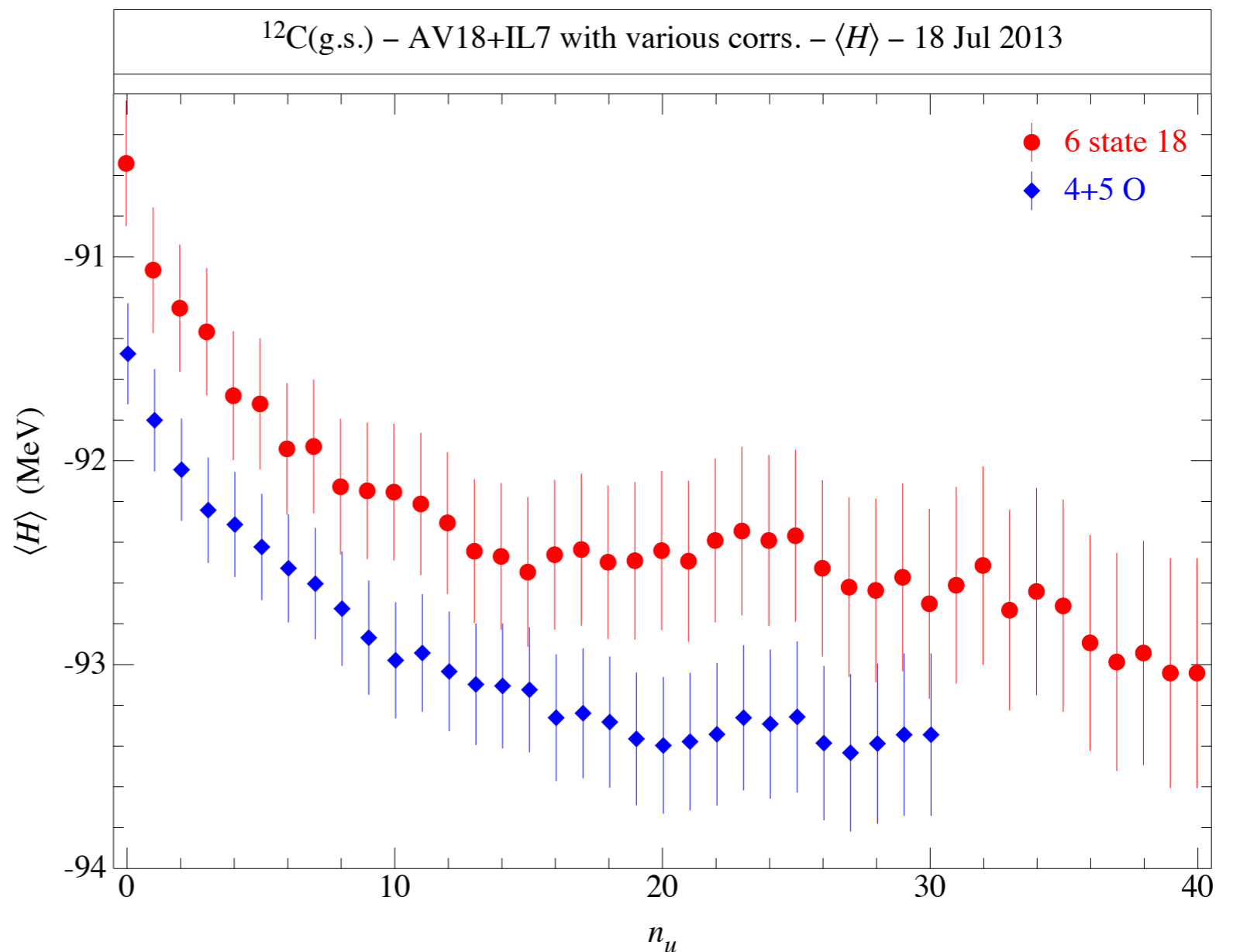
Green's Function Monte Carlo

Each path consists of a set of *n* steps, where each step contains a sample of 3*A* particle coordinates, as well as sets of operator orders used to sample the symmetrization operators $\mathcal{S}$ for the pair operators in the trial wave function.

To control the sign problem, an algorithm for discarding configurations which resembles as much as possible the constrained-path algorithms is implemented.

The algorithm has been tested studying the dependence upon constraining wave function and also the convergence of the results obtained by relaxing the constraint.

^{12}C(g.s.) – AV18+IL7 with various corrs. – $\langle H \rangle$ – 18 Jul 2013

6 state 18
4+5 O

$\langle H \rangle$ (MeV)

n_u

Need to go beyond MPI

- The branching process of the GFMC algorithm involves replication and killing of the samples, the number of which can undergo large fluctuations.

- In the original version of the code, several Monte Carlo samples, say at least 10, were assigned to each rank.

Rank 1	10	12	11	9
Rank 2	10	8	9	12
Rank 3	10	11	13	8
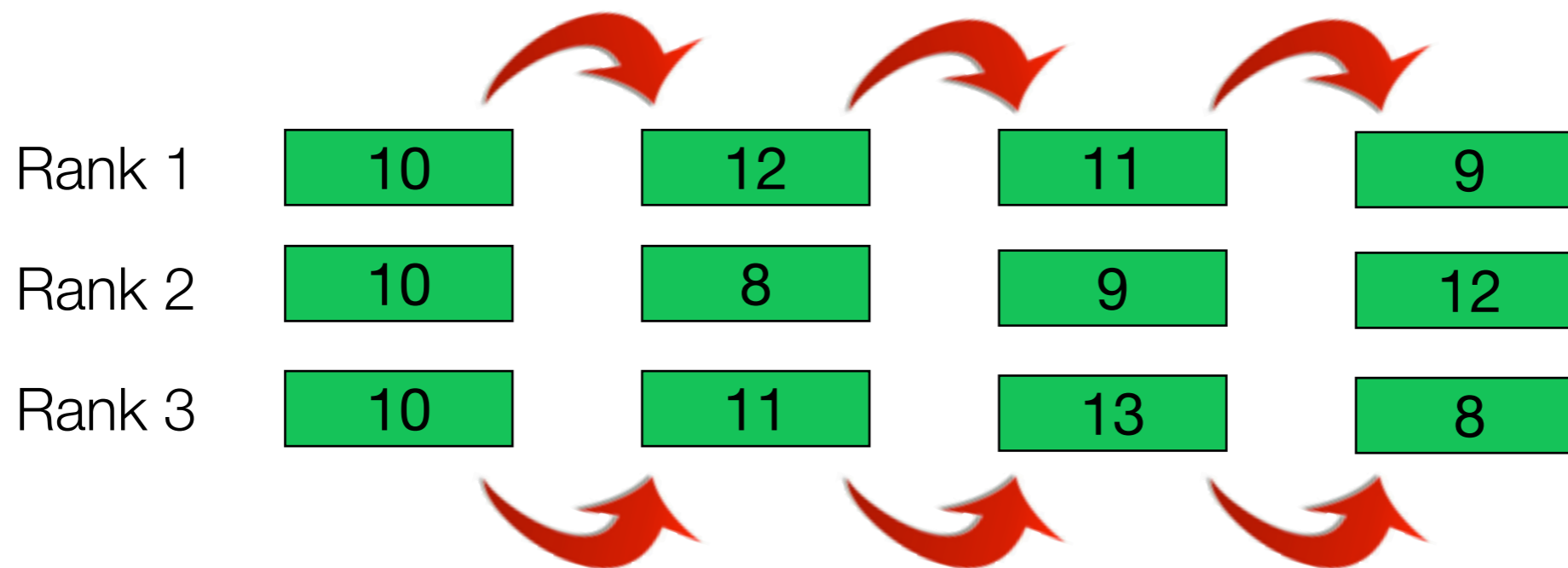
- A typical ^{12}C calculation involves around 15,000 samples while leadership class computers have many 10,000's of processors, making the algorithm quite inefficient.

ADLB library: overview

• Nodes are organized in servers and slaves; in standard GFMC calculations approximately 3% of the nodes are ADLB servers.


🟡 Application Processes

🟢 ADLB Servers

put/get
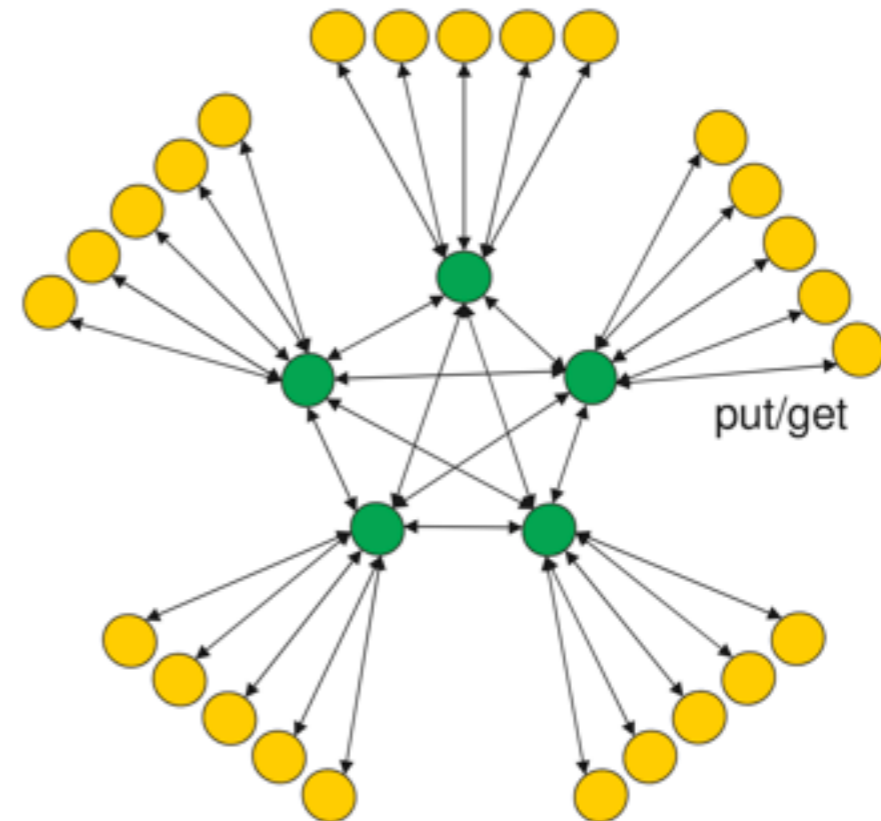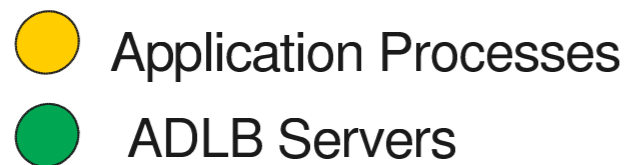
• A shared work queue, managed by the servers, is accessed by the slaves that either put work units, denoted as "work packages" in it or get those work packages out to work on them.

• Once a work package has been processed by a slave, a "response package" may be sent to the slave that put the work package in the queue.

ADLB library: implementation

- In order to reduce the statistical error associated with GFMC, the sum rules and the longitudinal form factor are evaluated for:

12 directions of the momentum transfer
(in four groups of three orthogonal directions)

21 values of the discretized momentum
transfer magnitude
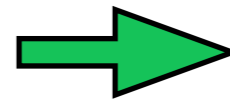
→ 252 independent
expectation values
need to be computed.

- The evaluation of the sum rules of the ^{12}C for a single value of the momentum transfer takes of about 360 seconds (with 16 OpenMP threads)

- ADLB is used to split the calculation in such a way that each slave calculates the sum rules and the form factor for a single value of $\mathbf{q}$.

ADLB library: implementation

• The response work package contains the left and right wave functions and, in certain cases, their derivatives.

```fortran
TYPE respon_wp_package_der
    sequence
! common part of package
    complex(8), dimension(nspin0, niso1) :: cfl, cfr
    complex(4), dimension(ns,niso1,3,npart0) :: cfdl, cfdr
    real(8) :: rpart0(3*npart0)
    real(8) :: actf, weight
    integer(4) :: iptb, if2, ijunk
    logical(4) :: prtsw
! variable part
    real(8), dimension(3) :: qh
    real(8) :: q
    integer(4) :: iqq, iqh
END TYPE respon_wp_package_der
```

As big as 1.30 GB !
Impossible on Intrepid!

• ADLB solution

Common part put: called once for each configuration.

```fortran
call ADLB_Begin_batch_put(rwp%cfl, respon_wp_len_common, ierr)
```

Variable part put: called for each q.

```fortran
call ADLB_PUT(rwp%qh, respon_wp_len_var, -1, myid, adlbwp_respon, i_prior, ierr)
```
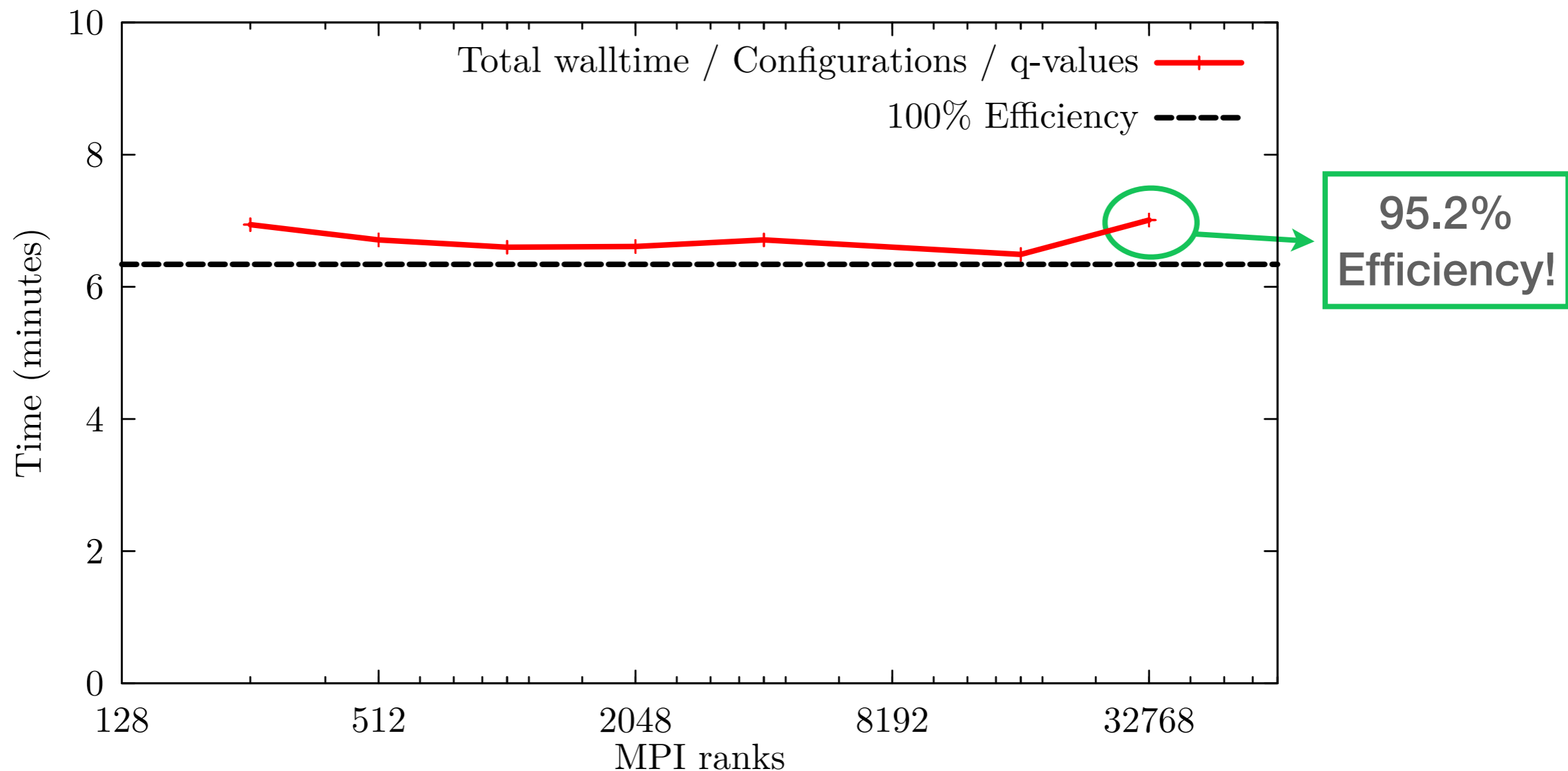
ADLB library: performance

- Very good scaling of the energy calculation up to 262,144 MPI ranks!

^{12}C – GFMC+ADLB – BG/Q

Weak scaling, 2 configs/rank
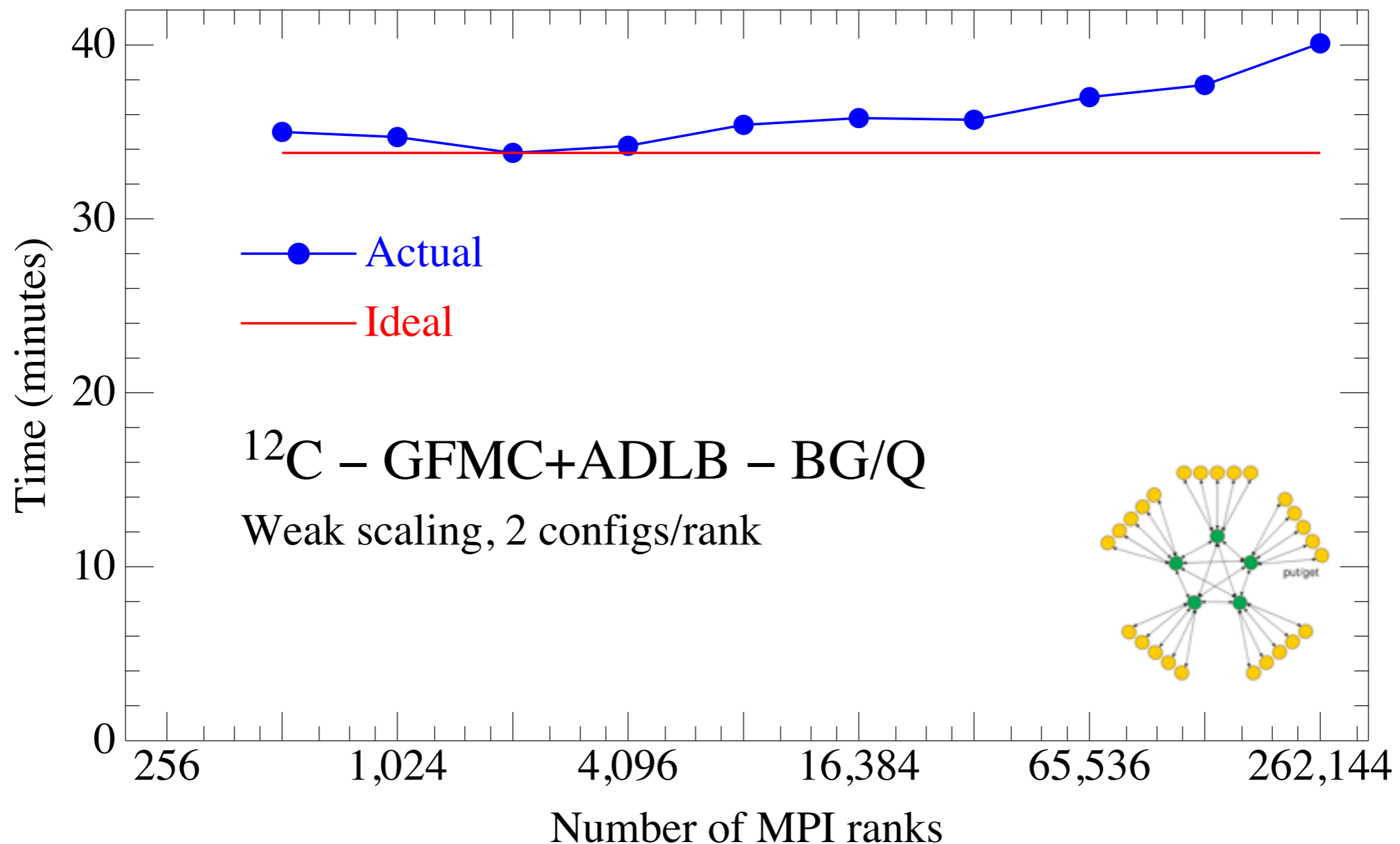
ADLB library: performance

- Very good scaling of the calculation: total time per configuration per q-value very close to the ideal case.

Results - Longitudinal form factor

- Experimental data are well reproduced by theory over the whole range of momentum transfers;

- Two-body terms become appreciable only for q > 3 fm^{-1}, where they interfere destructively with the one-body contributions bringing theory into closer agreement with experiment.
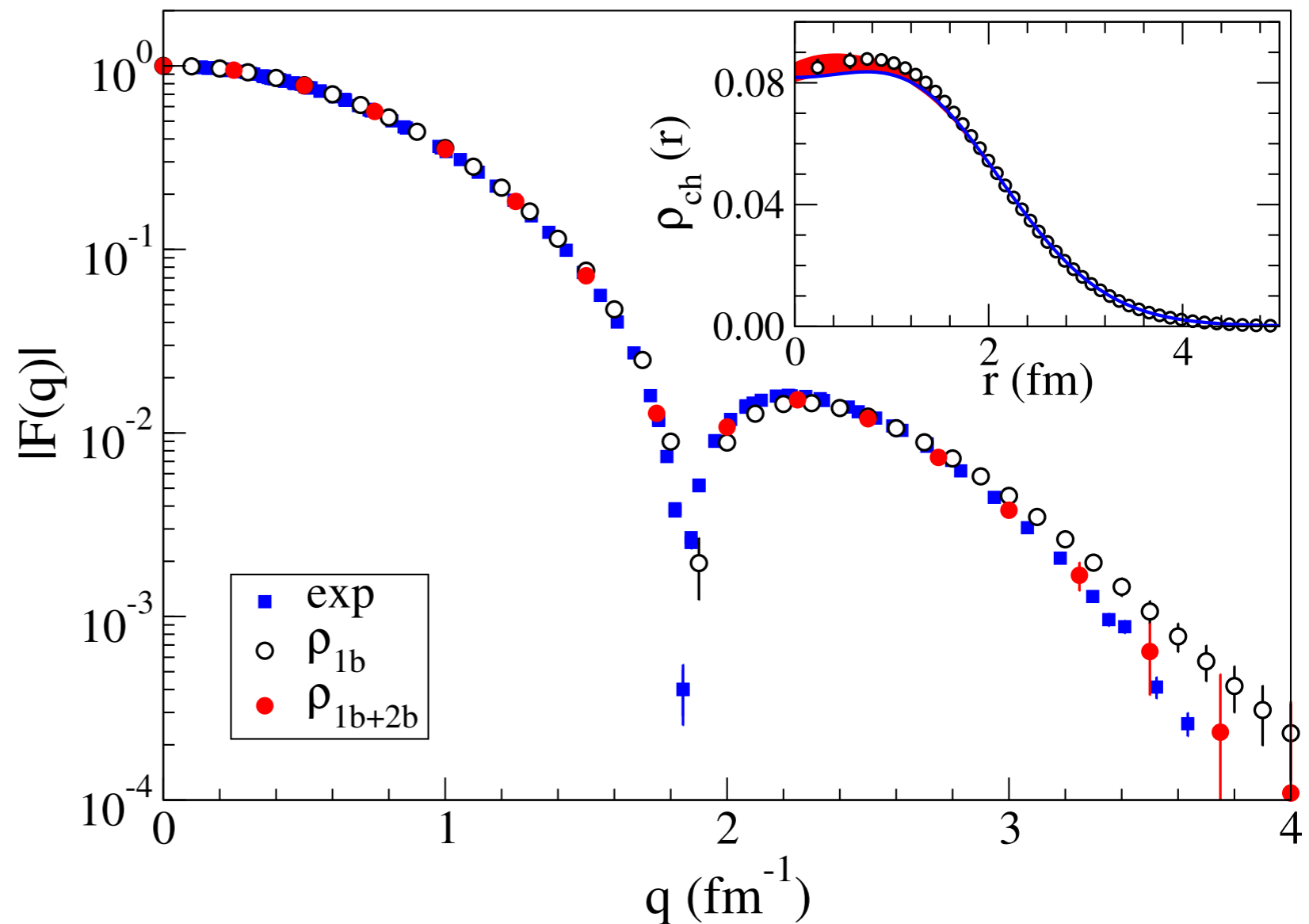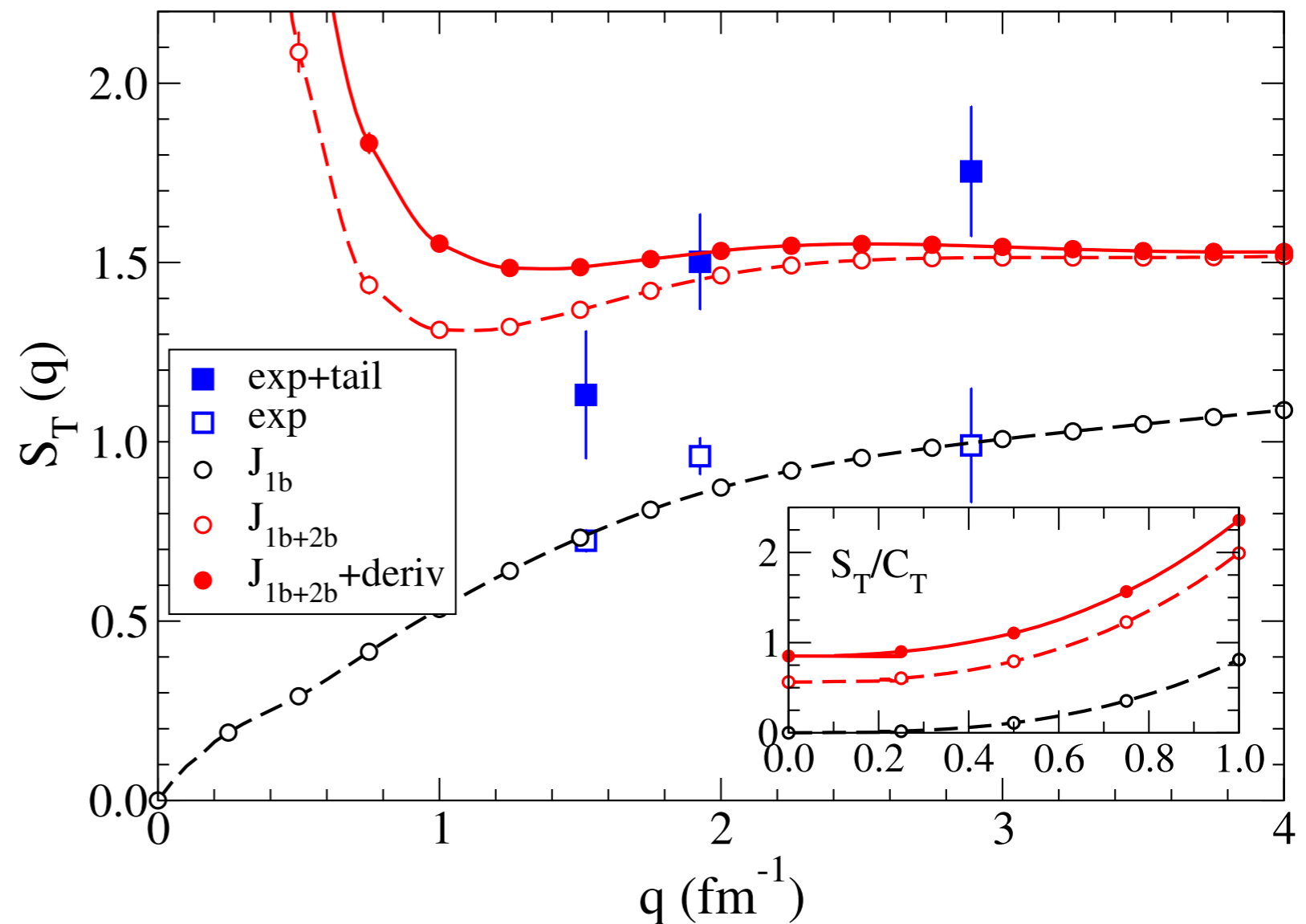
Results - Longitudinal sum rule

- S_L vanishes quadratically at small momentum transfer.

- The one-body sum rule in the large q limit differs from unity because of relativistic correction and convection term.

- Satisfactory agreement with the experimental values, including tail contributions.

- No significant quenching of longitudinal strength is observed
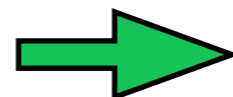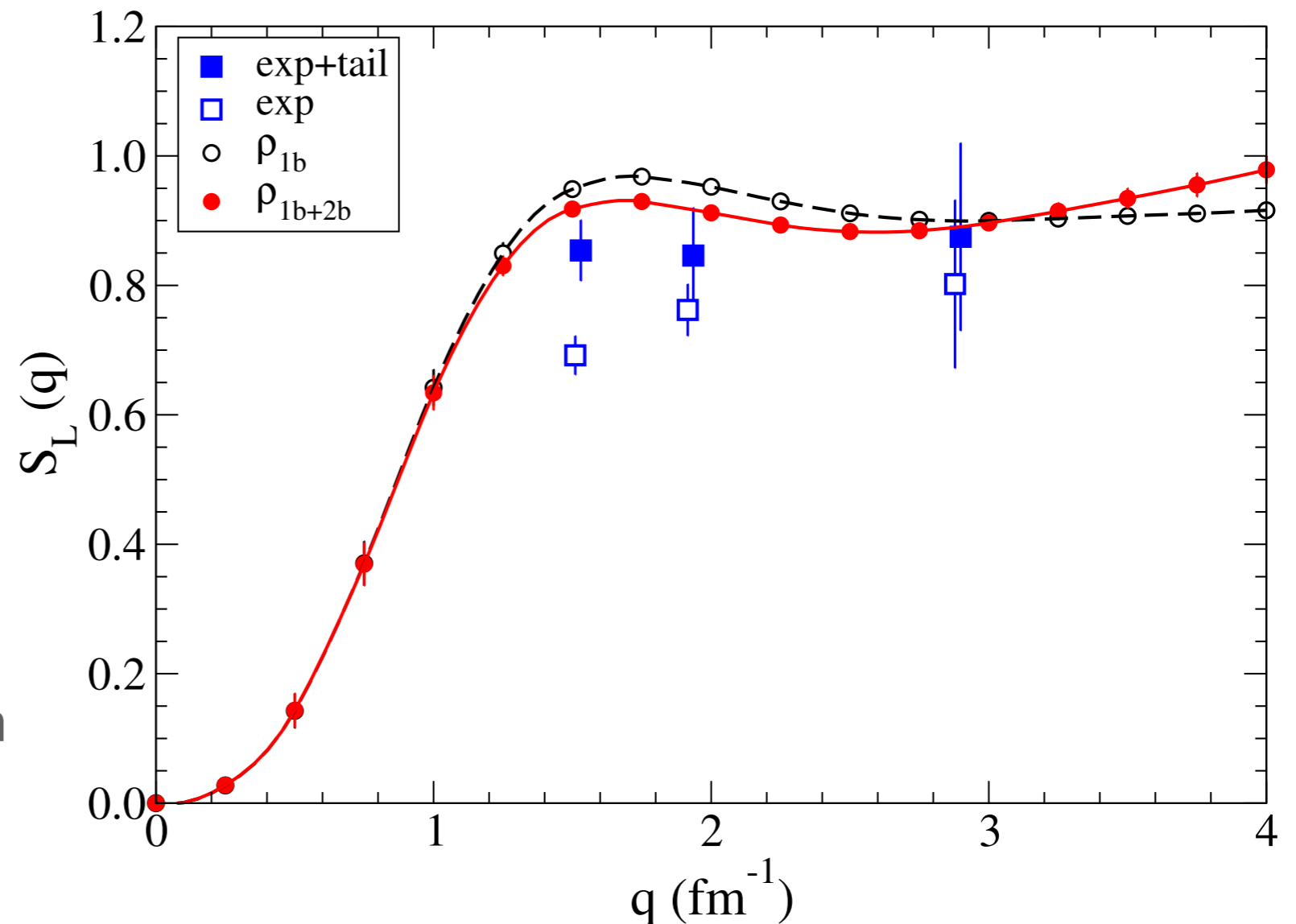
No evidence for significant in-medium modifications of the nucleon electromagnetic form factors.

Results - Transverse sum rule

- Divergent behavior at small q due to the normalization factor C_T.

- Comparison with experimental data made difficult by the Δ peak.

- Large two-body contribution, most likely from the quasi-elastic region, needed for a better agreement with experimental data.

Conclusions

• Very good description of the longitudinal form factor; two body terms bring theory into closer agreement with experiment.

• As for the longitudinal sum rule, we find satisfactory agreement with the experimental values, including tail contributions. Hence, we find no evidence for in-medium modifications of the nucleon electromagnetic form factors.

• In the transverse sum rule large two-body contribution the sizable contribution of the two-body terms is needed for a better agreement with experimental data.

• Very good ADLB scaling up to 32,768 ranks (at least), using 4 ranks per node.

• Good OpenMP scaling in each process: using 16 threads (the most possible) instead of only 4 reduces the time per configuration per q-value from about 12 to 6 minutes

Future

- Neutral current sum rules, allowing for the description of neutrino scattering on Carbon-12, are currently being implemented in the code.

- Euclidean electromagnetic response calculation of 12-carbon

$$E_\alpha(\mathbf{q}, \tau) = \int_{\omega_{th}}^{\infty} e^{-(\omega - E_0)\tau} R_\alpha(q, \omega)$$

will enable us to make a more direct comparison with data. Its implementation does not involve conceptual difficulties, as it consists in the evaluation of matrix elements like

$$M(\tau) = \frac{\langle 0|O_\alpha^\dagger e^{-(H - E_0)\tau} O_\alpha|0\rangle}{\langle 0|e^{-(H - E_0)\tau}|0\rangle}$$

Future

The ^{4}He transverse sum rule (not divided by the form factor) of the response function exhibits a sizable enhancement due to two-body terms.